Cerebral Cortex February 2009;19:424–434
doi:10.1093/cercor/bhn093
Advance Access publication June 11, 2008

Dopamine Innervation in the Thalamus: Monkey versus Rat

Miguel Ángel García-Cabezas, Patricia Martínez-Sánchez, Miguel Ángel Sánchez-González, Miguel Garzón and Carmen Cavada

Departamento de Anatomía, Histología y Neurociencia, Facultad de Medicina, Universidad Autónoma de Madrid, 28029 Madrid, Spain

We recently identified the thalamic dopaminergic system in the human and macaque monkey brains, and, based on earlier reports on the paucity of dopamine in the rat thalamus, hypothesized that this dopaminergic system was particularly developed in primates. Here we test this hypothesis using immunohistochemistry against the dopamine transporter (DAT) in adult macaque and rat brains. The extent and density of DAT-immunoreactive (-ir) axons were remarkably greater in the macaque dorsal thalamus, where the mediodorsal association nucleus and the ventral motor nuclei held the densest immunolabeling. In contrast, sparse DAT immunolabeling was present in the rat dorsal thalamus; it was mainly located in the mediodorsal, paraventricular, ventral medial, and ventral lateral nuclei. The reticular nucleus, *zona incerta*, and lateral habenular nucleus held numerous DAT-ir axons in both species. Ultrastructural analysis in the macaque mediodorsal nucleus revealed that thalamic interneurons are a main postsynaptic target of DAT-ir axons; this suggests that the marked expansion of the dopamine innervation in the primate in comparison to the rodent thalamus may be related to the presence of a sizable interneuron population in primates. We remark that it is important to be aware of brain species differences when using animal models of human brain disease.

Keywords: dopamine, macaque, rat, species differences, thalamus

Introduction

Dopamine is an important neurotransmitter in mammalian brain function, most notably in motor control, motivation and cognition. Dopamine dysfunction is key to human neurological and psychiatric disorders, including Parkinson's disease, schizophrenia and drug addiction (Di Chiara 2002). The dopaminergic systems thought to have roles in these disorders, that is, the mesostriatal, mesolimbic, and mesocortical, are the focus of considerable research attention. However, what is a conspicuous thalamic dopaminergic system was only identified recently by our group in monkey and human brains (Sánchez-González et al. 2005; García-Cabezas et al. 2007). We assumed that perhaps the reported paucity of dopaminergic axons in the rat thalamus (Groenewegen 1988; Papadopoulos and Parnavelas 1990) may have hindered earlier recognition of the abundant dopamine innervation in the primate thalamus even though considerable scattered evidence supported its presence (reviewed in García-Cabezas et al. 2007). It should be pointed out that the published rat studies were based on immunohistochemistry against dopamine, and this technique is technically difficult and of limited sensitivity (Groenewegen 1988; Papadopoulos and Parnavelas 1990; García-Cabezas et al. 2007). In our laboratory, dopamine immunohistochemistry in monkeys has provided useful information mainly to assess the very dense innervation of the thalamic midline nuclei (Sánchez-González et al. 2005; García-Cabezas et al. 2007), where most of the axons come from dopaminergic neurons that do not express the dopamine transporter (DAT) (Sánchez-González et al. 2005). However, most of the data we gathered on the distribution of dopaminergic axons in the primate thalamus relied on immunohistochemistry against DAT, which is very sensitive and a specific marker of the dopaminergic phenotype (Ciliax et al. 1999).

Considering the above evidence, we reasoned that the dopamine innervation of the rat thalamus warranted a re-examination using the sensitive DAT-immunolabeling technique available nowadays. Also, another question is whether rodents actually are a useful study model to investigate the role of the thalamic dopaminergic system in conditions linked to dopamine dysfunction. We therefore designed the present study to compare the thalamic dopamine innervation in the macaque monkey and rat brains. We used DAT immunohistochemistry in parasagittal sections of both species and in coronal rat brain sections. Thus we were able to collect information on the distribution of DAT-immunoreactive (-ir) axons in the rat thalamus, and complement the information on the distribution of the dopamine innervation in the macaque thalamus that we had mapped on coronal sections in previous studies (García-Cabezas et al. 2007). Moreover, by examining the ultrastructure of the DAT-ir axons in the macaque mediodorsal thalamic nucleus (MD) it has been possible to identify their postsynaptic targets.

Materials and Methods

Subjects and Tissue Preparation

The parasagittal maps of the thalamus in Figures 1 and 2 are derived from the right hemispheres of an adult male *Macaca fascicularis* monkey weighing 3.5 kg, and of an adult male Sprague–Dawley rat weighing 305 g. The left hemisphere from the same rat, sectioned in the parasagittal plane, and the brains of 2 additional male rats, weighing 300 and 350 g, and sectioned in the coronal plane, were also processed and analyzed under the light microscope. One of these rat brains had received injections of fluorescent axonal tracers in the left striatum and thalamus prior to perfusion. The thalamic injections were very small and did not impair the DAT immunoreaction, and so the intact hemithalamus and most of the injected hemithalamus were available for study.

The ultrastructural analysis was performed on tissue from 2 adult male *Macaca mulatta* monkeys weighing 7.9 and 4.5 kg. The left hemisphere from one of these monkeys was a gift from Dr Uwe Ilg and Dr Peter Thier, University of Tübingen, Germany. The right hemisphere from this animal had been used for electrophysiological recordings and subsequent injection of the various axonal tracers in different cortical areas: diamidino yellow in the middle temporal visual area, fast blue in the medial superior temporal visual area, cholera toxin b-subunit conjugated to colloidal gold in the frontal eye field, biotinylated dextran amine in the supplementary eye field and horseradish peroxidase conjugated to wheat germ agglutinin in the lateral intraparietal area. It

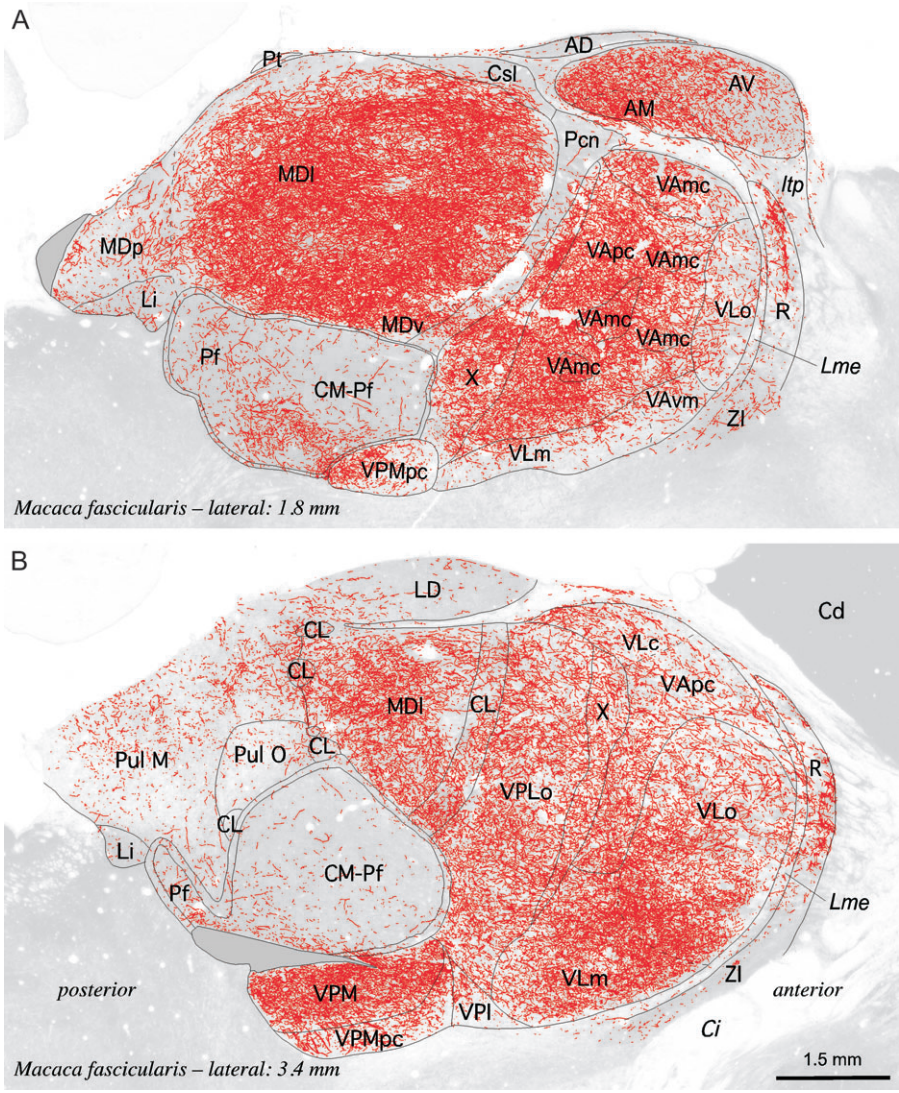

Figure 1. Distribution of DAT-ir axons (red) in parasagittal sections of the macaque monkey thalamus. DAT-ir axons are presented over micrographs of adjacent sections stained for AChE activity, which were the main reference for identifying the thalamic nuclei. The AChE micrographs were rendered partially transparent to attenuate contrast and facilitate visualization of the DAT-ir axons. The lateral distance from the midline is given for each section; anterior is to the right and posterior to the left. Note the marked differences in DAT-ir axonal density between the various nuclei, with the MD nucleus (the lateral sector in the figure —MDl—) and the ventral thalamic nuclei holding the densest immunolabeling. The plain grey zones in A and B correspond to tissue regions damaged in the immunoreacted sections. The calibration bar applies to (A) and (B). AD, anterodorsal nucleus; AM, anteromedial nucleus; AV, anteroventral nucleus; Cd, caudate nucleus; *Ci*, internal capsule; CL, central lateral nucleus; CM-Pf, centromedian-parafascicular complex; Csl, central nucleus-superior lateral part; *ltp*, inferior thalamic peduncule; LD, lateral dorsal nucleus; Li, limitans nucleus; *Lme*, external medullary lamina; MDl, mediodorsal nucleus-lateral sector; MDv, mediodorsal nucleus-ventral sector; MDp, mediodorsal nucleus-posterior sector; Pcn, paracentral nucleus; Pf, parafascicular nucleus; Pt, parataenial nucleus; Pul M, medial pulvinar nucleus; Pul O, oral pulvinar nucleus; R, reticular nucleus; VAmc, ventral anterior nucleus-magnocellular part; VApc, ventral anterior nucleus-parvocellular part; VAvm, ventral anterior nucleus-ventromedial part; VLc, ventral lateral nucleus-caudal part; VLm, ventral lateral nucleus-medial part; VLo, ventral lateral nucleus-oral part; VPl, ventral posterior inferior nucleus; VPLo, ventral posterior lateral nucleus-oral part; VPM, ventral posterior medial nucleus; VPMpc, ventral posterior medial nucleus-parvocellular part; X, ventral lateral nucleus-area X; ZI, *zona incerta*.

is very unlikely that these tracers interfered with the DAT immunolabeling carried out in the thalamus of the opposite hemisphere because 1) crossed thalamo-cortical projections from the MD to the macaque prefrontal and temporo-parietal cortices are not thought to exist (Preuss and Goldman-Rakic 1987; Boussaoud et al. 1992; Cavada and Goldman-Rakic 1993); 2) the very limited crossed corticothalamic projection from the prefrontal cortex to MD targets the dorsomedial angle of the nucleus (Preuss and Goldman-Rakic 1987); neither the prefrontal cortex proper, nor its contralalateral MD target zone were injected or sampled in the animal used in the present study. In fact, the features of DAT immunolabeling observed in the MD from the naïve animal and from the one that had received axonal tracer injections in the opposite hemisphere were similar (see below), indicating that in actuality the tracers did not affect the findings in the present study.

Animal handling followed Spanish and European guidelines (Boletín Oficial del Estado of 18 March 1988, and 86/609/EEC and 2003/65/EC European Council Directives) and was approved by the Committee for Research Ethics of the Universidad Autónoma de Madrid.

Following deep anesthesia, the animals were perfused through the heart and ascending aorta with saline, a fixation solution and a series of buffered sucrose solutions for cryoprotection as described earlier (Sánchez-González et al. 2005; García-Cabezas et al. 2007). The fixation solution contained 4% paraformaldedyde in all animals except one of the monkeys, which was fixed with a mixture of 4% paraformaldehyde and 0.2% glutaraldehyde for ultrastructural analysis.

The monkey and rat hemispheres to be used for light microscopy were frozen-sectioned at 40 μm in the parasagittal or coronal planes. The hemispheres to be used for electron microscopy were blocked in

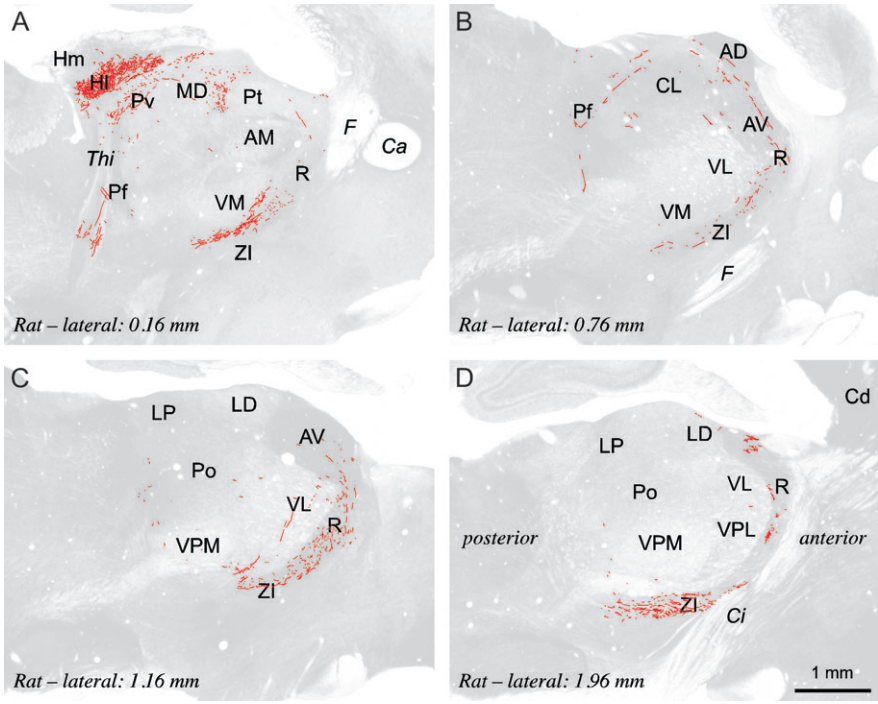

Figure 2. Distribution of DAT-ir axons (red) in parasagittal sections of the rat thalamus. DAT-ir axons are presented over micrographs of nearby sections stained for AChE activity that reveal the various thalamic nuclei; these micrographs were rendered partially transparent to attenuate contrast and facilitate visualization of the DAT-ir axons. The lateral distance from the midline is given for each section; anterior is to the right, and posterior to the left in all sections. Note the paucity of immunolabeling in the dorsal thalamic nuclei and compare with the noticeable and extensive labeling in the dorsal thalamic nuclei of the monkey thalamus presented in Figure 1. In the rat, the structures most densely labeled are outside the dorsal thalamus: thalamic reticular nucleus (R), *zona incerta* (ZI), and lateral habenular nucleus (Hl). The calibration bar applies to (A)-(D). AD, anterodorsal nucleus; AM, anteromedial nucleus; AV, anteroventral nucleus; *Ca*, anterior commissure; Cd, caudate nucleus; *Ci*, internal capsule; CL, central lateral nucleus; *F*, fornix; Hm, medial habenular nucleus; LD, lateral dorsal nucleus; LP, lateral posterior nucleus; MD, mediodorsal nucleus; Pf, parafascicular nucleus; Po, posterior nucleus; Pt, parataenial nucleus; Pv, paraventricular nucleus; *Thi*, habenulo-interpeduncular tract; VL, ventral lateral nucleus; VM, ventral medial nucleus; VPL, ventral posterior lateral nucleus; VPM, ventral posterior medial nucleus.

the coronal plane; slabs from the thalamus were dissected and then sectioned in a vibratome at 40 μm. In all cases, series of adjacent sections were collected. One series was always processed for acetylcholinesterase (AChE) activity, which is particularly useful to identify the thalamic nuclei (Paxinos and Watson 1986; Cavada et al. 1995). An additional series from the monkey and rat hemispheres to be used for mapping was stained with cresyl violet for cytoarchitectural reference. The remaining series were stored at –20 °C in an ethylene-glycol buffered solution or used for DAT immunostaining.

Immunohistochemistry

DAT immunostaining was performed on free-floating sections as described earlier in detail (Sánchez-González et al. 2005; García-Cabezas et al. 2007). Thus, only a brief account is given here.

The monkey and rat tissue to be examined under the light microscope was subject to microwave antigen retrieval prior to immunostaining in order to optimize the immunolabeling. The monkey and rat parasagittal sections used for mapping were immunoreacted together to maximize the comparability of the data; the remaining rat tissue was immunoreacted in independent experiments using the same protocol. The coronal sections used for electron microscopy were incubated in a cryoprotectant solution (25% sucrose and 3% glycerol in 0.05 M phosphate buffer) for 50 min and then rapidly freeze-thawed by immersion in liquid nitrogen to enhance the penetration of immunoreagents. Thereafter, these sections underwent the same immunohistochemical procedure as the tissue for light microscopy, save for the complete omission of Triton X-100 in the incubations. The primary antibody was MAB369, a rat monoclonal supplied by Chemicon International (Temecula, CA). This antibody corresponds to the DAT/Nt antibody generated against human DAT N-terminus aminoacids 1–66 by Ciliax et al. (1995), who demonstrated its specificity using immunoblot analysis, immunoprecipitation, preadsorption followed by immunoblotting and immunohistochemistry, and several immunohistochemical assays. MAB369 was used at a 1:1000 dilution. The secondary antiserum was AP164B, a biotinylated rabbit anti-rat antiserum, from the same company, used at a 1:400 dilution. The sections were incubated in Vectastain Elite avidin/biotin complex from Vector Labs (Burligame, CA) prior to peroxidase development. The sensitive glucose oxidase–diaminobenzidine–nickel method (Shu et al. 1988) was used to develop the rat and monkey sections to be examined under the light microscope. A standard diaminobenzidine protocol (0.05% diaminobenzidine and 0.003% H_2O_2) was used to develop the monkey sections to be processed for ultrastructural analysis.

In all immunostaining sessions, negative control sections containing structures rich in DAT, like the caudate nucleus, were run in parallel with the experimental sections. In the negative controls, the primary antibody was omitted from the protocol. No immunolabeling was observed in these negative control sections. Positive control tissue included the ventral tegmental area, *substantia nigra*, and caudate nucleus, which were present in many of the experimental sections (e.g. Figs 1*B*, 2*D*). As expected, the DAT-rich centers were densely stained in the experimental sections from both monkeys and rats.

Electron Microscope Methods

Three vibratome sections from the thalamus of 2 monkeys were DAT immunoreacted, postfixed in 1% osmium tetroxide for 60 min, and dehydrated through a graded series of ethanol and propylene oxide. These sections were incubated overnight in a 1:1 mixture of propylene oxide and Epon resin (EM bed-812; Electron Microscopy Sciences, Fort Washington, PA), transferred to Epon 100% for 2–3 h, flat-embedded between 2 sheets of Aclar plastic film, and cured in an oven at 58 °C for 72 h. Small portions (approx. 3–4 mm^2) of the MD nucleus were selected using a dissecting magnifying microscope, cut from the sections and glued onto resin blocks. Ultrathin tissue sections (40–60 nm) were cut

from the outer surface of the blocks and collected on copper mesh grids. The sections were counterstained for 4 min with 5% uranyl acetate in methanol followed by a solution containing 0.022 mg of lead citrate in 0.5 mL of NaOH 1 N and 4.5 mL of distilled water.

Data Analysis

The monkey and rat sections processed for light microscopy were examined with a Zeiss Axioskop microscope (Oberkochen, Germany). The DAT-ir axons present in the parasagittal monkey and rat sections were drawn using a Neurolucida set-up (MicroBrightField, Colchester, VT) attached to another Zeiss Axioskop microscope as described earlier (García-Cabezas et al. 2007). The borders of the diencephalon and blood vessels were drawn over the immunostained sections and were then superimposed onto the AChE sections so that the borders of the thalamic nuclei could be traced. As well, the cresyl violet sections were routinely used to identify the thalamic nuclei; they were particularly useful for distinguishing the various monkey ventral nuclei. In addition to our earlier studies on AChE activity in the monkey thalamus (Cavada et al. 1995), reference atlases were used to identify the monkey and rat thalamic nuclei (Olszewski 1952; Paxinos and Watson 1986; Ilinsky and Kultas-Ilinsky 2002). The nomenclature used for the thalamic nuclei is based on Olszewski (1952); nuclei specific to the rat thalamus are named following Paxinos and Watson (1986). The micrographs of Figures 1–4 were made with a digital camera (AxioCam HRc, Zeiss, Germany) mounted onto a Zeiss Axiophot microscope (Oberkochen, Germany).

The ultrastructural analysis was conducted with a Jeol JEM 1010 electron microscope. Electron micrographs at 20 000× and 40 000× magnifications were taken with a digital camera (BioScan—GATAN, Pleasanton, CA) and saved in TIFF format. The micrographs were from ultrathin sections collected near the surface of the tissue at the interface with the Epon embedding resin. The MD regions examined included the lateral (MDl) and medial sectors of the nucleus. The classification of cellular profiles was based on the descriptions of Peters et al. (1991). Dendrites were identified by the presence of postsynaptic densities and/or an abundance of endoplasmic reticulum and microtubules. Axons were recognized by their small caliber, smaller than any dendritic profile, and by their lack of ribosomes. When sectioned transversely, axons had smooth contours and were often grouped in bundles. Axons cut longitudinally usually displayed varicosities with vesicles. Synapses were defined as either symmetric or asymmetric depending on the respective presence of thin or thick postsynaptic specializations. Nonsynaptic contacts or appositions were defined as close membranous associations that lacked recognizable specializations. A neuronal profile was considered to be selectively labeled with immunoperoxidase when the precipitate made it appear more electron dense than morphologically similar profiles observed within the same section. All DAT-ir profiles were identified based on the morphological characteristics of the tissue and the presence of DAT immunolabeling. The diameter, perimeter and surface area of the DAT-ir profiles were measured using the public domain NIH ImageJ 1.33 program (developed at the US National Institutes of Health and available on the Internet at http://rsb.info.nih.gov/nih-image/).

Canvas X software (ACD Systems, Miami, FL) was used to build and label all the Figures. Retouching of the micrographs included gray scale rendering (Figs 1–4), transparency adjustments (Figs 1 and 2), and small changes of brightness and contrast.

Results

Distribution of DAT-ir Axons in the Monkey and Rat Thalamus

Figure 1 shows the distribution of *macaque* DAT-ir axons superimposed onto micrographs of the adjacent AChE-stained sections. Note the uneven distribution of the labeling throughout the various nuclei, as well as within individual nuclei like the MD or the oral part of the ventral lateral (VL) nucleus. The densest immunolabeling was in the association MD nucleus (MDl sector in Fig. 1, see also Fig. 3*A*) and in several ventral motor nuclei, including the magnocellular and parvocellular parts of the ventral anterior (VA) nucleus, the oral, caudal, and medial parts of the VL nucleus, area X, and the oral part of the ventral posterior lateral nucleus (VPLo). Lower densities of DAT-ir axons were present in the anterior nuclear group as a whole, in particular in the anteromedial (the most densely innervated within the anterior group) and anteroventral (AV) nuclei, in the intralaminar central lateral (CL) nucleus and centromedian–parafascicular (CM–Pf) complex (where the -ir axons are concentrated in the parafascicular nucleus -Pf-), and in the medial pulvinar nucleus. The anterodorsal nucleus, lateral dorsal nucleus, the anterior intralaminar paracentral nucleus, the midline nuclei paratenial (Pt) and central-superior, lateral part, and nucleus limitans showed very low immunostaining. These observations are broadly in keeping with our earlier descriptions based on coronal sections from the thalamus of *Macaca nemestrina* (Sánchez-González et al. 2005; García-Cabezas et al. 2007). In addition, conspicuous immunolabeling was present in the region of the ventral posterior medial nucleus (VPM) lying ventral to the CM–Pf complex, and in the parvocellular VPM (VPMpc) (Fig. 1*B*). The marked immunolabeling in the ventral VPM region was unexpected; in previous studies, the VPM nucleus showed weak immunostaining (Sánchez-González et al. 2005; García-Cabezas et al. 2007). The ventral VPM region mapped in the present study was not included in the previous monkey maps. It holds the trigeminal representation of ipsilateral inner mouth mucous surfaces: fauces, palate, mouth floor, and tongue (Rausell and Jones 1991). It appears that this ventral VPM region and the adjacent gustatory VPMpc are more innervated by DAT-expressing axons than the more lateral parts of VPM that hold the representation of facial and scalp skin. Nevertheless, it should be noted that VPMpc and the ventral VPM contain many thick DAT-ir axons, sometimes grouped in bundles, that appear to cross the nucleus in a ventro-dorsal direction (Fig. 4). Thus, the density of DAT-ir axons mapped in these nuclei in Figure 1*B* is somewhat misleading as it reflects the presence of many axons of passage in addition to thin varicose axons possibly innervating the neuronal populations of VPMpc and the ventral VPM region.

Outside the dorsal thalamus, significant DAT-ir labeling was present in the reticular nucleus (R) (Fig. 3*C*) and in the *zona incerta* (ZI).

Figure 2 shows the distribution of DAT-ir axons throughout the *rat* thalamus. The sections selected for illustration were those with the most extensive DAT immunolabeling. Comparison with Figure 1 shows that the rat thalamus is quite poor in DAT-ir axons as compared with the monkey thalamus. The nuclei holding the densest immunolabeling in rats were not in the dorsal thalamus proper; rather, the epithalamic lateral habenular nucleus (Hl) held the densest immunolabeling (Fig. 2*A*), followed by the ventral thalamic R nucleus (Figs 2*B–D* and 3*D*) and the ZI. Within the dorsal thalamus the following nuclei showed low densities of DAT-ir axons: the midline paraventricular (Pv), the MD (Fig. 3*B*), and the ventral nuclei ventral medial (VM) and VL (Fig. 2*A–C*). Scattered DAT-ir axons were present in Pt, AV, CL, and Pf. We paid particular attention to the lateral geniculate nucleus (GL) because earlier reports demonstrated the presence of dopamine-ir axons there (Papadopoulos and Parnavelas 1990). However, we were unable to detect DAT-ir axons in any of the 6 rat GL nuclei examined.

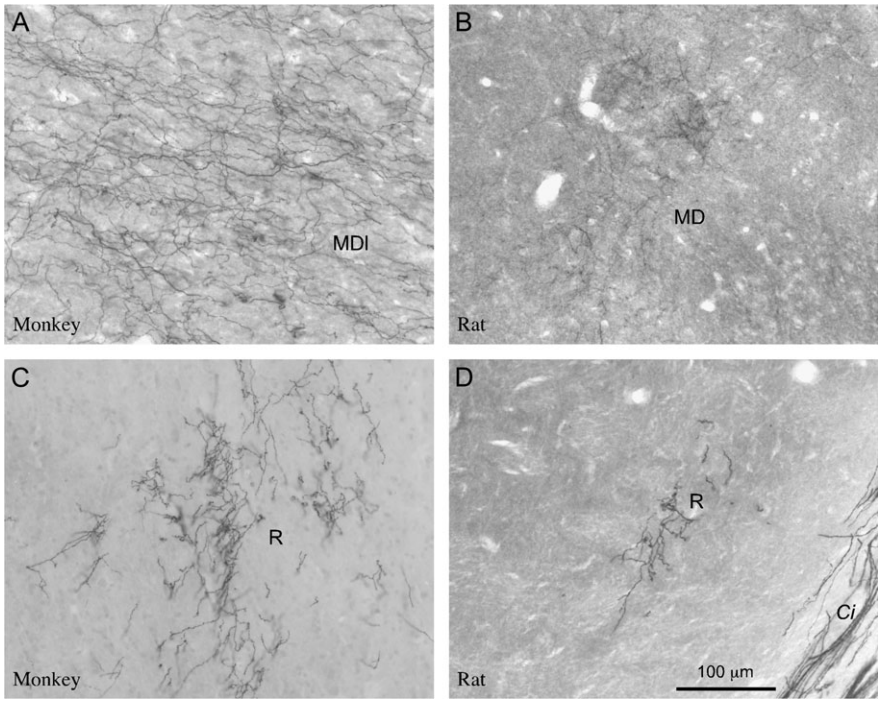

Figure 3. Micrographs of representative thalamic nuclei holding DAT-ir axons (black) in the monkey and rat thalamus. The rat fields shown are those with the densest immunolabeling in the rat thalamus; they correspond to the MD labeling mapped in Figure 2*A* and the reticular nucleus (R) labeling shown in Figure 2*D*. In the monkey thalamus notably more extensive labeling was present in MD and R, as represented also in Figure 1. *Ci*, internal capsule. The calibration bar applies to (*A*)–(*D*).

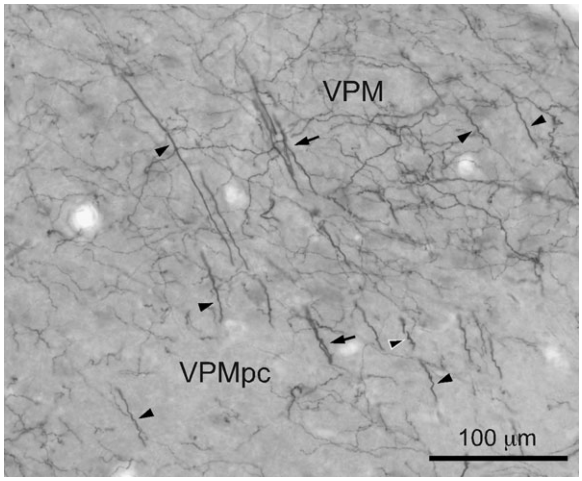

Figure 4. Photomicrograph of DAT-ir axons (black) in the monkey VPM region lying ventral to the CM–Pf complex, and in the VPMpc. Note the presence of many thick DAT-ir axons in both nuclei that are either isolated (black arrowheads) or grouped in bundles (black arrows). Some of the thick DAT-ir axons show a ringlet-like shape (black arrowhead outlined in white). The thick DAT-ir axons, possibly representing passing axons, are mixed with the typical thin varicose axons prevalent in most other thalamic nuclei.

We wish to note that the DAT immunoreaction in the rat hemisphere selected for mapping was optimal, as confirmed, in particular, in the mesencephalon and cerebral cortex. In the frontal and cingulate cortices from the same sections represented in Figure 2, DAT-ir axons were intensely stained; in fact they were far more easily detected than in the thalamus where their thin diameters made them somewhat difficult to detect. The findings from the 2 rat brains sectioned in the coronal plane agreed with those illustrated in Figure 2. All considered, we conclude that the reduced DAT immunolabeling present in the rat thalamus as compared with the monkey thalamus is a genuine finding and not a technical artifact.

Ultrastructure of Macaque DAT-ir Axons

All DAT-ir axons were unmyelinated, varicose, and very thin (Fig. 5); they were all in the extraglomerular neuropil of MD, and, when cut longitudinally, they had a tortuous and irregular course. DAT immunoreaction product showed a discrete localization to restricted segments of the axons: it was present either in intervaricose spaces or in varicose enlargements, but was not detected in terminal enlargements (*boutons terminaux*). No differences were observed between the 2 monkeys examined (n = 227 and 67 axons, respectively); thus, their data were pooled.

The majority of the DAT-ir axons (82%) showed the immunoperoxidase reaction product apposed to the inner surface of the plasmalemma, as well as in the cytoplasm, vesicles and other organelles (Fig. 5*A*,*B*). In two-thirds of these axons, the DAT-ir was prominently associated to the plasma membrane, that is, apposed the inner surface of the plasmalemma along portions of variable length, and was intensely electron dense. We name this pattern of labeling DAT-Type I (Fig. 5*A*). The remaining one-third of the axons with immunoperoxidase apposed to the plasmalemma showed a preferential localization of the DAT immunoprecipitate within the cytoplasm and axonal organelles. We name this pattern of labeling DAT-Type II (Fig. 5*B*). Overall, the immunoprecipitate was paler in axons with DAT-Type II than in those with DAT-Type I immunolabeling. DAT-Type I and DAT-Type II labeling patterns were present in 62% and 20%, respectively, of the studied axon population. In the remaining

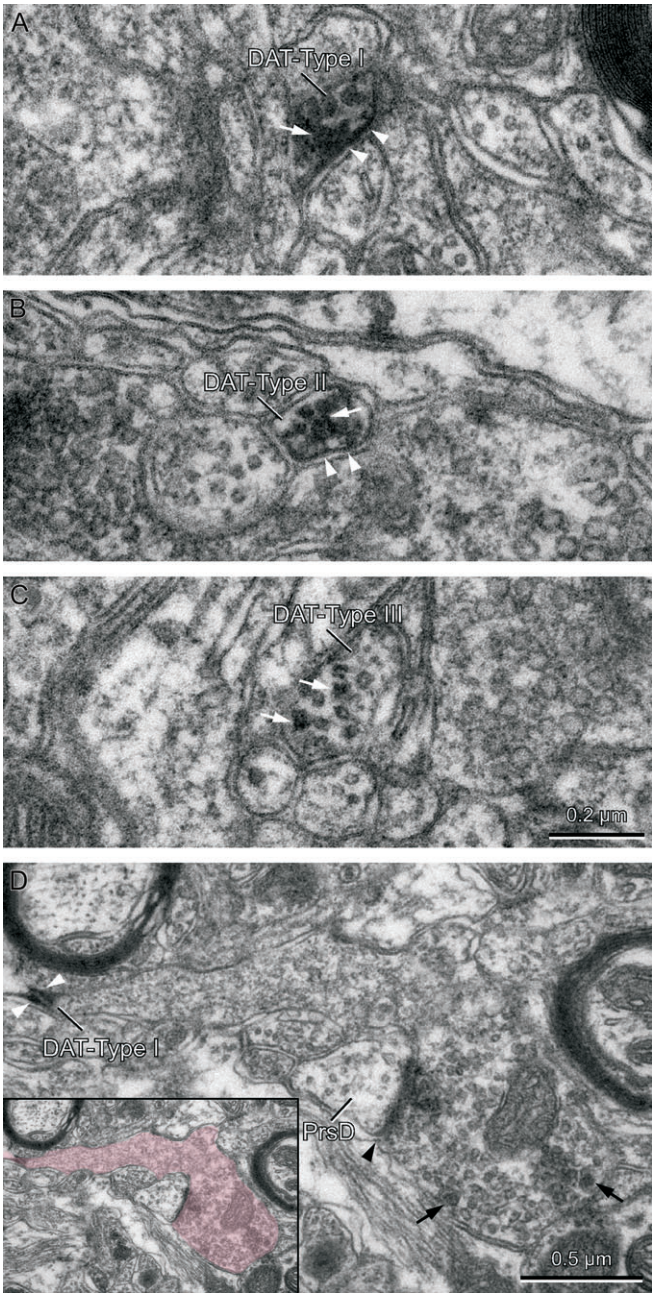

Figure 5. Ultrastructure of DAT-ir axons in the macaque MD. (*A*–*C*) Transversely cut inmunolabeled axons showing the 3 types of labeling we identified. (*D*) Longitudinally cut immunolabeled axon with its terminal endowed with vesicles and a synaptic profile (identified in color in the inset). White arrows in (*A*)–(*C*) point to immunoprecipitate in the cytoplasm and axonal organelles. White arrowheads in (*A*), (*B*), and (*D*) point to immunoprecipitate rimming the inner border of the plasma membrane, a feature present in DAT-Type I and DAT-Type II immunolabeling patterns. DAT-Type I immunolabeling is characterized by intensely electron dense immunoprecipitate conspicuously attached to the plasma membrane (*A* and *D*), whereas DAT-Type II immunolabeling is characterized by the immunoprecipitate preferentially located within the cytoplasm and its organelles (*B*). In the DAT-Type III immunolabeling pattern, the immunoprecipitate is confined to the cytoplasm and mostly associated to microtubules (*C*). The axon in D establishes a synaptic contact (black arrowhead) that is located far from the DAT immunoperoxidase product (white arrowheads). The axon terminal contains many synaptic vesicles, some of them with dense cores (black arrows). Note the presence of vesicles in the postsynaptic element, thus identified as a presynaptic dendrite (PrsD), typical of thalamic interneurons. The calibration bar in (*C*) applies to (*A*)–(*C*).

18% of the axons, the immunolabeling was located within the cytoplasm and mostly associated to microtubules, whereas the plasmalemma was devoid of immunoprecipitate. We name this pattern of labeling DAT-Type III (Fig. 5*C*).

The mean cross-section diameter of axons with DAT-Type I immunolabeling was 0.13 μm (SD = 0.04), their mean perimeter was 0.81 μm (SD = 0.29), and mean surface area was 0.04 μm^2 (SD = 0.02). The mean diameter of axons with DAT-Type II immunolabeling was 0.16 μm (SD = 0.07), their mean perimeter was 0.96 μm (SD = 0.50), and mean surface area was 0.06 μm^2 (SD = 0.06). The mean diameter of axons with DAT-Type III immunolabeling was 0.17 μm (SD = 0.06), their mean perimeter was 0.88 μm (SD = 0.34), and mean surface area was 0.05 μm^2 (SD = 0.03). Because in cross-section a mean diameter may include measurements of both varicosities and intervaricose segments, we also measured the diameters of varicosities and intervaricose segments in longitudinally cut DAT-ir axons (n = 70). The mean diameter of varicosities for axons with DAT-Type I, DAT-Type II and DAT-Type III labeling patterns was 0.16 μm (SD = 0.05), 0.16 μm (SD = 0.05), and 0.16 μm (SD = 0.02), respectively; and the mean diameter of intervaricose segments was 0.08 μm (SD = 0.05), 0.09 μm (SD = 0.04), and 0.08 μm (SD = 0.03), respectively. This indicates that the diameters of varicosities and intervaricose segments in axons with DAT-Type I, DAT-Type II, and DAT-Type III labeling patterns are similar and that the measurements made in cross-section probably contained a larger number of varicosities for axons with DAT-Type II and DAT-Type III patterns than for axons with DAT-Type I labeling pattern.

Very few membrane contacts (n = 9) were observed in the population of macaque DAT-ir axons analyzed. Most contacts (n = 7) occurred in axons with DAT-Type I immunolabeling. *Bona fide* synaptic junctions with clear membrane specializations were observed in 5 axons with DAT-Type I immunolabeling and in one axon with DAT-Type II immunolabeling; 5 of these synaptic junctions were asymmetric (4 in axons with DAT-Type I immunolabeling, one in the axon with the DAT-Type II immunolabeling) and one was a symmetric contact (in an axon with DAT-Type I immunolabeling). In most cases the immunoprecipitate appeared distant from the synaptic contact (Fig. 5*D*), at a mean distance of 0.49 μm (SD = 0.38) for the asymmetric synapses. In the one synapse identified as symmetric the immunoprecipitate was located next to the synaptic contact. In all synaptic contacts, the postsynaptic profile was a dendrite with vesicles (Fig. 5*D*); this is characteristic of presynaptic dendrites from thalamic interneurons, including those of the macaque MD (Schwartz et al. 1991; Schwartz and Mrzljak 1993). No axo-somatic contacts were observed. Finally, 2 axons with DAT-Type I immunolabeling and one with DAT-Type II immunolabeling established appositional contacts without membrane specializations, classified as *puncta adherens*. The contacted profile was, in 2 cases, a dendrite devoid of vesicles, thus presumed to be a projection neuron dendrite, and, in the third case, by an axon with DAT-Type I immunolabeling, it was a dendrite with vesicles, which was thus identified as an interneuron dendrite.

Discussion

The main finding from the present study is that the dopamine innervation of the thalamus, as evidenced by DAT immunostaining, is markedly denser and more widespread in the

macaque monkey than in the rat. This finding confirms our presumption of a thalamic dopaminergic system especially developed in primates that was inferred from independent reports and based on findings using different methodologies applied to the primate (Sánchez-González et al. 2005; García-Cabezas et al. 2007) and the rat (Groenewegen 1988; Papadopoulos and Parnavelas 1990). In addition, the present ultrastructural analysis shows that, in the macaque MD nucleus, DAT is located in very thin unmyelinated axons at a distance of several tenths of a micron from synaptic terminals. These DAT-expressing axons appear to target mostly thalamic interneurons.

DAT-Expressing Axons in the Macaque and Rat Thalamus. Species Differences

The present data on the distribution of thalamic DAT-ir axons in parasagittal sections from *M. fascicularis* largely confirm our earlier descriptions based on coronal sections from *Macaca nemestrina* and *M. mulatta*: the DAT-expressing axons are unevenly distributed between the different nuclei and within individual nuclei, and the thalamic nuclei receiving the densest innervation from DAT-expressing axons are the association MD nucleus and motor ventral nuclei, including VA, VL, and VPLo. Two additional thalamic territories, not included in the present monkey maps, are also densely innervated by dopamine: the association lateral posterior (LP) nucleus, which holds a dense innervation by DAT-expressing axons, and the midline nuclei, which hold a dense dopamine innervation mostly from axons either devoid of or poor in DAT (Sánchez-González et al. 2005; García-Cabezas et al. 2007). Other thalamic nuclei show moderate or low dopamine innervation (Fig. 1).

The different densities of the dopamine innervation in the primate thalamic nuclei are expressed in Figure 6 by different intensities of red. In light of the dopamine innervation in the thalamic nuclei and the tight connections between thalamus and cortex, it follows that the cortical regions most influenced by thalamic dopamine are the prefrontal and motor cortices, which themselves receive a strong direct dopamine innervation (Williams and Goldman-Rakic 1993; Lewis et al. 2001), and dorsal portions of the posterior parietal cortex (Fig. 6; see review of primate thalamo-cortical connections of the nuclei with high or moderate dopamine innervation in Table 1 of García-Cabezas et al. 2007). The cingulate cortex and large territories of parieto-occipito-temporal association cortex would be moderately influenced by thalamic dopamine while the primary sensory areas would be the least influenced (Fig. 6). The present data provide, however, an exception to this general scheme: the primary gustatory cortex and the nearby primary somatosensory cortex where the inner mouth mucosa is represented (located in the frontal operculum and adjacent anterior parietal cortex—Krubitzer et al. 1995; Hirata et al. 2005; Miyamoto et al. 2006; Smits et al. 2007), receive connections from thalamic nuclei that appear moderately innervated by DAT-expressing axons, specifically, from VPMpc and the ventral part of VPM (Figs 1 and 4).

In marked contrast with the prominent presence of DAT-expressing axons in the monkey thalamus, the rat thalamus holds only limited clusters of axons and scattered axons that express DAT (Fig. 2). Our findings of DAT-positive axon clusters in the Pv and MD nuclei, and in the Hl, are consistent with the reported presence of dopamine-ir fibers in these nuclei (Groenewegen 1988) and with changes described in rat

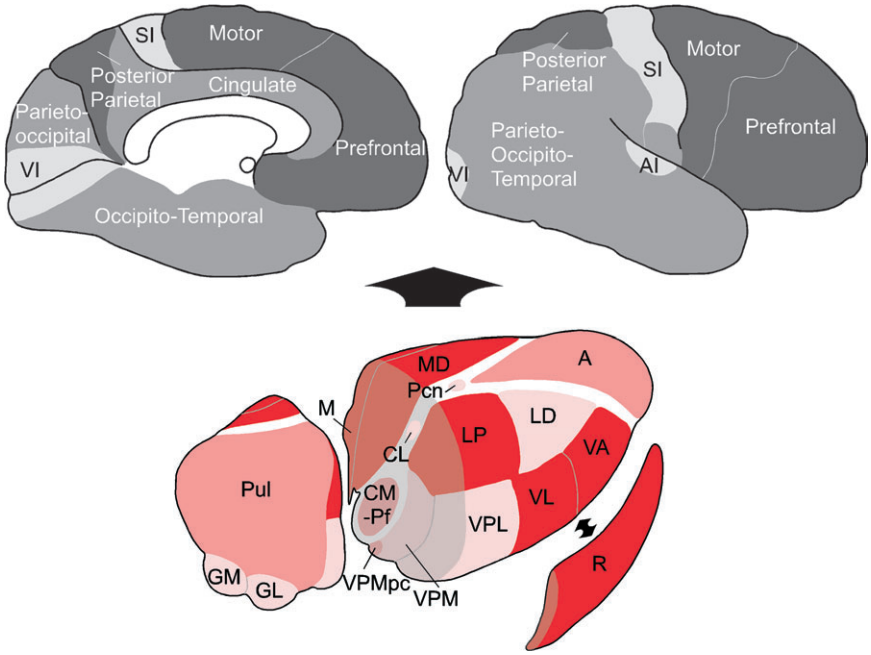

Figure 6. Influence of thalamic dopamine on primate cortical function as inferred from the density of the dopamine innervation in the thalamus (represented by three different intensities of red) and from the organization of thalamo-cortical connections. The cortical regions receiving input from the most densely dopamine innervated thalamic nuclei are represented in the darkest gray color to indicate the impact of thalamic dopamine on their corresponding functional domains. These regions include the prefrontal and motor cortices and part of the posterior parietal cortex. In contrast, the cortical areas receiving input from the thalamic nuclei with the least dopamine innervation are shown in the lightest gray shade and correspond to the primary visual (VI), auditory (AI), and somatosensory (SI) areas. A, anterior group of nuclei; CL, central lateral nucleus; CM-Pf, centromedian-parafascicular complex; GL, lateral geniculate nucleus; GM, medial geniculate nucleus; LD, lateral dorsal nucleus; LP, lateral posterior nucleus; M, midline group of nuclei; MD, mediodorsal nucleus; Pcn, paracentral nucleus; Pul, pulvinar nuclei; R, reticular nucleus; VA, ventral anterior nucleus; VL, ventral lateral nucleus; VPL, ventral posterior lateral nucleus; VPM, ventral posterior medial nucleus; VPMpc, ventral posterior medial nucleus-parvocellular part.

MD neuron membrane properties following D2 receptor stimulation (Lavin and Grace 1998). In the present study we also found substantial DAT immunolabeling in the rat R nucleus and ZI, and clusters of DAT-ir axons in the VM and VL ventral nuclei, and scattered DAT-ir axons in Pt, AV, CL, and Pf. The presence of DAT-ir axons in the rat Pv, Hl and R concurs with tract-tracing studies reporting projections to these nuclei from dopaminergic neurons of the fore-and/or midbrain (Takada et al. 1990; Li et al. 1993; Anaya-Martinez et al. 2006). However, we did not observe DAT-ir axons in the GL, where dopamine-ir axons have been reported (Papadopoulos and Parnavelas 1990), and a number of studies have shown that delivery there of dopamine or dopamine-receptor agonists has an effect on neuronal activity (Albrecht et al. 1996; Govindaiah and Cox 2005; Munsch et al. 2005). It is possible that dopaminergic axons in the GL nucleus, if present, are devoid of DAT or express it below the threshold level for our methods. It should be borne in mind that not all dopaminergic neurons express DAT (Sánchez-González et al. 2005); that, among those expressing it, levels are variable (Haber et al. 1995; Sánchez-González et al. 2005); and that some dopaminergic cell groups, specifically A8 through A11, hold a mixed population of cell bodies that, being dopaminergic, are either DAT-positive or DAT-negative (Table 1 in Sánchez-González et al., 2005). Tract-tracing data in the monkey show that the thalamus receives projections from both dopaminergic DAT-positive and DAT-negative neurons. In the midline nuclei, for example, the majority of the dopaminergic axons come from hypothalamic and lateral parabrachial dopaminergic cell groups that do not express DAT; the non-midline nuclei, which make up most of the thalamic volume, however, receive the bulk of their afferent dopaminergic input from DAT-expressing cell groups (Sánchez-González et al. 2005). It is possible, then, that the rat GL nucleus receives dopaminergic input from neurons that do not express DAT. Examination of the origin of the dopaminergic axons targeting the rat thalamic nuclei, including GL, would help to settle if the latter receives a dopamine innervation. In addition, it would help to clarify if the origin of the dopamine innervation of the rat thalamus comes from such a diverse collection of dopaminergic cell groups as in the monkey, which includes groups that express DAT, as in the mesencephalon, and those that are devoid of DAT expression, as in the hypothalamus (Sánchez-González et al. 2005).

The observed expansion in extent and density of the dopamine innervation in the primate versus the rodent dorsal thalamus deserves comment. The general layout of dopaminergic cell groups is comparable in the primate and rodent brains although dopaminergic neurons are more widely distributed in the primate than in the rodent mesencephalon (Kitahama et al. 1994; Verney 1999). The general distribution of dopaminergic terminals in the striatum is also similar (Reiner 1994; Ciliax et al. 1995; Ciliax et al. 1999). In the cerebral cortex, however, the patterns of regional and laminar distribution of dopaminergic axons differ significantly between primates and rodents. In rats, dopamine innervation is present mainly in the prefrontal, anterior cingulate, insular, piriform, entorhinal, and perirhinal cortices, with the posterior cingulate, motor, parietal, and temporal cortices being lightly innervated. Dopaminergic terminals in the rat cortex are distributed in deep layers with the exception of the anterior cingulate and entorhinal cortices where they are present in deep and superficial layers (Berger et al. 1991; Ciliax et al. 1995). In primates the dopamine innervation in the cerebral cortex is expanded and differently distributed: it targets all cortical areas, is densest in the motor cortices, and is present in the deep and superficial layers with the molecular layer being the most densely innervated in all areas (Berger et al. 1991; Williams and Goldman-Rakic 1993; Ciliax et al. 1999; Lewis et al. 2001). Thus, it appears that the major differences in dopamine innervation between the rodent and primate brains are in the cerebral cortex and dorsal thalamus (present report and García-Cabezas et al. 2007).

Moreover, there seems to be a correlation between the relative densities of dopaminergic axons in the primate cortex and thalamus, with cortical regions heavily innervated by dopamine connected with densely innervated thalamic nuclei (i.e., motor, prefrontal, and posterior parietal areas; ventral motor, MD, and LP thalamic nuclei), and poorly innervated cortical regions linked with dopamine poor thalamic nuclei (e.g., primary visual cortex; GL nucleus). Thus, the wider and denser dopamine innervation in the primate dorsal thalamus as compared with the rodent may parallel the expansion of the mesocortical dopaminergic system noted by Berger and Gaspar (1994) in relation to encephalization.

Finally, it is opportune to add that the notable differences in dopamine innervation between the dorsal thalamus of monkeys and rats are not evident in the ventral thalamus and epithalamus: the R, ZI, and Hl all show conspicuous innervation by dopamine in the human, monkey and rat brains (present data and García-Cabezas et al. 2007).

Ultrastructure and Targets of Thalamic DAT-Expressing Axons in the Monkey

The nearly 300 DAT-ir axons identified here in the monkey MD were unmyelinated, varicose and very thin, less than 0.1 μm in diameter. They were located in the extraglomerular neuropil and, based on the characteristics of the immunoprecipitate, we identified 3 immunolabeling patterns. In 82% of the axons the immunoprecipitate was apposed to the inner plasmalemma surface (this defined the DAT-Type I and DAT-Type II immunolabeling patterns, distinguished by their intense or pale immunoprecipitate, respectively); in the remaining 18% of the axons the immunoprecipitate was confined to the cytoplasm and was mostly linked to microtubules (DAT-Type III immunolabeling). These observations expand those reported using DAT and tyrosine hydroxylase immunohistochemistry in the macaque MD (Melchitzky et al. 2006). Melchitzky and colleagues concluded that the ultrastructure of DAT-ir axons in the MD is more similar to that of DAT-ir axons in the cortex than in the striatum. Indeed the mean diameters of DAT-ir axons in the monkey prefrontal cortex are in the range of the DAT-ir axons identified here in MD: 0.14 and 0.15 μm in prefrontal areas 46 and 9, respectively (Lewis et al. 2001); 0.08–0.09 μm and 0.16 μm for intervaricose segments and varicosities, respectively, in MD (present data). Nevertheless, the notion that the mesocortical and thalamic dopaminergic systems are associated because they share ultrastructural features requires a stronger justification and testing. For example, it remains to be determined if the dopaminergic axons in the cortex and thalamus, or a fraction of them, share a common nuclear origin, or may even be collaterals from the same neurons. This hypothesis is tenable because dopaminergic neurons from mesencephalic groups A8, A9, and A10 project to the motor and prefrontal cortices (Gaspar et al.

1992; Williams and Goldman-Rakic 1998) as well as the thalamus (Sánchez-González et al. 2005).

In the relatively large number of labeled axons examined here we were able to identify 6 synaptic junctions, 5 asymmetric and one symmetric, and their corresponding postsynaptic profiles. In all cases, the latter showed the features of presynaptic dendrites on a thalamic interneuron. Identification of synapses and postsynaptic profiles in catecholaminergic axons of the monkey thalamus has been elusive. We have identified them in only 2% of the DAT-immunolabeled axons, mostly within the population of axons that were cut longitudinally. Despite the low numbers, the present data represent the largest number of synaptic contacts identified to date in thalamic dopaminergic axons. In previous studies only 3 (Liu and Jones 1991) and 2 (Melchitzky et al. 2006) synaptic profiles were observed, all in tyrosine hydroxylase immunolabeled axons; and hence, they were only putatively dopaminergic. Among these 5 synapses the postsynaptic element was identified in only 3 cases: it was a dendritic shaft in 2 (Liu and Jones 1991; Melchitzky et al. 2006) and a presynaptic dendrite in the third case (Melchitzky et al. 2006). Apart from the number of axons analyzed, which should be high enough to provide a sizable number of synaptic forms, a main reason for the paucity of data on synapses and postsynaptic targets of catecholaminergic fibers in the monkey thalamus may lie in the plane of section. In our material synaptic specializations appeared at a mean distance of about 0.5 μm from the DAT immunoprecipitate; for this reason axons cut longitudinally are more likely to display synaptic specializations. In the monkey MD, most DAT-ir axons follow a rostro-caudal course (Fig. 1) and thus the coronal plane of section used so far (Melchitzky et al. 2006; present study) renders mostly transversely cut axons (76% of the total DAT-ir axons in our material); the parasagittal plane of section should render more longitudinally cut axons and would thus be more appropriate for the analysis of dopaminergic synapses. Another technical means to refine and increase the identification of synaptic profiles in dopaminergic axons would be the use of serial sections. Future exhaustive ultrastructural analyses may uncover further details of the morphological relationships between dopaminergic axons and their targets in the monkey thalamus.

The subcellular location of the DAT immunoprecipitate, and the identification in the present study of the interneurons as the predominant postsynaptic element in the monkey MD are worth consideration. In most axons (82%) the DAT immunoprecipitate was apposed to the membrane, and when synapses were identified, the immunoprecipitate was located far from them (Fig. 5*D*). This suggests that in the macaque MD synaptically released dopamine may diffuse for considerable time and distance before being re-uptaken by DAT. This possibility is compatible with a "volume" or "extrasynaptic" transmission mode in the thalamic dopaminergic system comparable to that proposed for the mesostriatal and mesocortical systems (Pickel et al. 1996; Zoli et al. 1998; Lewis et al. 2001). The plausible existence of volume transmission would mean that the released dopamine may spread farther than the postsynaptic neurons, thus reaching projection neurons.

Finally, in the macaque MD the thalamic interneurons appear to be the main postsynaptic target of dopaminergic axons. The interneurons in the macaque MD account for 25% and 35% of the total neuronal population in the magnocellular and parvocellular sectors, respectively, of the nucleus (Clark et al. 1989). The proportion of thalamic interneurons in other monkey thalamic nuclei, including anterior, ventral, lateral and intralaminar nuclei, as well as GL, is within the same range as in MD (Montero and Zempel 1986; Hendry 1991; Hunt et al. 1991). In contrast, the rat thalamus is virtually devoid of interneurons, except for the lateral and medial geniculate and the LP nucleus (Ottersen and Storm-Mathisen 1984). It is thus tempting to hypothesize that the sizable interneuron population and the conspicuous population of dopaminergic axons targeting the interneurons evolved in parallel and are particularly prominent in the primate brain. Nevertheless, even if this hypothesis proves true, the uneven density of the dopamine innervation across the various primate thalamic nuclei remains to be explained. It is interesting, though, that uneven densities of dopamine innervation in the cortex and thalamus seem to coincide, and thus densely innervated cortical regions are connected with densely innervated thalamic territories.

Concluding Remarks

We have shown marked differences in the dopamine innervation of the thalamus between monkeys and rats. These species differences should be taken into account when considering the use of animals as models for human diseases coursing with dopamine dysfunction, in particular Parkinson's disease and schizophrenia. The presence of abundant DAT in the primate thalamus implies that the nuclei densely innervated by DAT-expressing axons may be important sites of action of toxins that selectively destroy dopaminergic neurons acting through DAT (Pifl and Caron 2002). One such toxin is 1-methyl-4-phenyl-1,2,3,6-tetrahydropyridine (MPTP), used to produce experimental parkinsonism in both primates and rodents (Pifl and Caron 2002). It is possible that in MPTP-treated monkeys the thalamic nuclei innervated by DAT-expressing axons are dopamine dennervated (see Pifl et al. 1990, 1991, for support of this hypothesis) and that a decrease in thalamic dopamine contributes to the pathophysiology of parkinsonism. Such pathogenic mechanism would hardly work in rats because their thalamic dopaminergic system is rudimentary.

The species differences shown here should also be considered in studies dealing with the effects on the brain of psychoactive drugs that act through DAT, like cocaine or the amphetamines (Pifl and Caron 2002), because the primate brain holds more specific sites of action for those drugs than the rodent brain, in particular in the cerebral cortex and thalamus.

Funding

Ministry of Education and Science of Spain grant (SAF2005-05380).

Notes

The gift of monkey tissue by Dr Uwe Ilg and Dr Peter Thier, University of Tübingen, Germany, is gratefully acknowledged. We thank Gemma De la Fuente, Begoña Rodríguez Menéndez, Rosa Sánchez Lozano, Covadonga Aguado Ballano, and Francisco Urbano for qualified technical assistance.

This manuscript was prepared following a presentation at the Kavli Symposium in Memoriam of Patricia S. Goldman-Rakic held in New

Haven, CT, USA, in May 2006. Carmen Cavada wishes to express her most sincere gratitude to Patricia Goldman-Rakic: Pat's mentorship at Yale University in the 1980s was decisive for my scientific career. Pat exposed me to the nonhuman primate brain; it was a privileged and exciting experience. Pat's influence is still having a protracted and extensive effect on the collaborators that have worked and are now working in my group, always with a focus on the primate brain. The professional collaboration between Pat and myself mingled and continued with a growing friendship. I value most what she taught me through her grace and attitudes: that each person has his talents, and that it is wise to discover, nurture and focus on them. It was a blessing to enjoy Pat's mentorship and amity. This article is dedicated to her memory. *Conflict of Interest*: None declared.

Address correspondence to Carmen Cavada, MD, PhD, Departamento de Anatomía, Histología y Neurociencia, Facultad de Medicina, Universidad Autónoma de Madrid, Arzobispo Morcillo s/n, 28029 Madrid, Spain. Email: carmen.cavada@uam.es.

References

Albrecht D, Quaschling U, Zippel U, Davidowa H. 1996. Effects of dopamine on neurons of the lateral geniculate nucleus: an iontophoretic study. Synapse. 23:70–78.

Anaya-Martinez V, Martinez-Marcos A, Martinez-Fong D, Aceves J, Erlij D. 2006. Substantia nigra compacta neurons that innervate the reticular thalamic nucleus in the rat also project to striatum or globus pallidus: implications for abnormal motor behavior. Neuroscience. 143:477–486.

Berger B, Gaspar P. 1994. Phylogeny and development of catecholamine systems in the CNS of vertebrates. Cambridge (UK): Cambridge University Press.

Berger B, Gaspar P, Verney C. 1991. Dopaminergic innervation of the cerebral cortex: unexpected differences between rodents and primates. Trends Neurosci. 14:21–27.

Boussaoud D, Desimone R, Ungerleider LG. 1992. Subcortical connections of visual areas MST and FST in macaques. Visual Neurosci. 9:291–302.

Cavada C, Compañy T, Hernández-González A, Reinoso-Suárez F. 1995. Acetylcholinesterase histochemistry in the macaque thalamus reveals territories selectively connected to frontal, parietal and temporal association cortices. J Chem Neuroanat. 8:245–257.

Cavada C, Goldman-Rakic PS. 1993. Multiple visual areas in the posterior parietal cortex of primates. Prog Brain Res. 95:123–137.

Ciliax BJ, Drash GW, Staley JK, Haber S, Mobley CJ, Miller GW, Mufson EJ, Mash DC, Levey AI. 1999. Immunocytochemical localization of the dopamine transporter in human brain. J Comp Neurol. 409:38–56.

Ciliax BJ, Heilman C, Demchyshyn LL, Pristupa ZB, Ince E, Hersch SM, Niznik HB, Levey AI. 1995. The dopamine transporter: immunochemical characterization and localization in brain. J Neurosci. 15:1714–1723.

Clark AS, Schwarz ML, Goldman-Rakic PS. 1989. GABA-immunoreactive neurons in the mediodorsal nucleus of the monkey thalamus. J Chem Neuroanat. 2:259–267.

Di Chiara G. 2002. Dopamine in the CNS. I & II. Berlin: Springer.

García-Cabezas MA, Rico B, Sanchez-González MA, Cavada C. 2007. Distribution of the dopamine innervation in the macaque and human thalamus. Neuroimage. 34:965–984.

Gaspar P, Stepniewska I, Kaas JH. 1992. Topography and collateralization of the dopaminergic projections to motor and lateral prefrontal cortex in owl monkeys. J Comp Neurol. 325:1–21.

Govindaiah G, Cox CL. 2005. Excitatory actions of dopamine via D1-like receptors in the rat lateral geniculate nucleus. J Neurophysiol. 94:3708–3718.

Groenewegen HJ. 1988. Organization of the afferent connections of the mediodorsal thalamic nucleus in the rat, related to the mediodorsal-prefrontal topography. Neuroscience. 24:379–432.

Haber SN, Ryoo H, Cox C, Lu W. 1995. Subsets of midbrain dopaminergic neurons in monkeys are distinguished by different levels of mRNA for the dopamine transporter: comparison with the mRNA for the D2 receptor, tyrosine hydroxylase and calbindin immunoreactivity. J Comp Neurol. 362:400–410.

Hendry SHC. 1991. Delayed reduction in GABA and GAD immunoreactivity of neurons in the adult monkey dorsal lateral geniculate nucleus following monocular deprivation or enucleation. Exp Brain Res. 86:47–59.

Hirata S, Nakamura T, Ifuku H, Ogawa H. 2005. Gustatory coding in the precentral extension of area 3 in Japanese macaque monkeys; comparison with area G. Exp Brain Res. 165:435–446.

Hunt CA, Pang DZ, Jones EG. 1991. Distribution and density of GABA cells in intralaminar and adjacent nuclei of monkey thalamus. Neuroscience. 43:185–196.

Ilinsky I, Kultas-Ilinsky K. 2002. Stereotactic atlas of the Macaca mulatta thalamus and adjacent basal ganglia nuclei. New York: Kluwer Academic.

Kitahama K, Nagatsu I, Pearson J. 1994. Catecholamine systems in mammalian midbrain and hindbrain: theme and variations. In: Smeets WJAJ, Reiner A, editors. Phylogeny and development of catecholamine systems in the CNS of vertebrates. Cambridge (UK): Cambridge University Press. p. 183–205.

Krubitzer L, Clarey J, Tweedale R, Elston G, Calford M. 1995. A redefinition of somatosensory areas in the lateral sulcus of macaque monkeys. J Neurosci. 15:3821–3839.

Lavin A, Grace AA. 1998. Dopamine modulates the responsivity of mediodorsal thalamic cells recorded in vitro. J Neurosci. 18:10566–10578.

Lewis DA, Melchitzky DS, Sesack SR, Whitehead RE, Auh S, Sampson A. 2001. Dopamine transporter immunoreactivity in monkey cerebral cortex: regional, laminar, and ultrastructural localization. J Comp Neurol. 432:119–136.

Li YQ, Takada M, Shinonaga Y, Mizuno N. 1993. The sites of origin of dopaminergic afferent fibers to the lateral habenular nucleus in the rat. J Comp Neurol. 333:118–133.

Liu X-B, Jones EG. 1991. The fine structure of serotonin and tyrosine hydroxylase immunoreactive terminals in the ventral posterior thalamic nucleus of cat and monkey. Exp Brain Res. 85:507–518.

Melchitzky DS, Erickson SL, Lewis DA. 2006. Dopamine innervation of the monkey mediodorsal thalamus: location of projection neurons and ultrastructural characteristics of axon terminals. Neuroscience. 143:1021–1030.

Miyamoto JJ, Honda M, Saito DN, Okada T, Ono T, Ohyama K, Sadato N. 2006. The representation of the human oral area in the somatosensory cortex: a functional MRI study. Cereb Cortex. 16:669–675.

Montero VM, Zempel J. 1986. The proportion and size of GABA-immunoreactive neurons in the magnocellular and parvocellular layers of the lateral geniculate nucleus of the rhesus monkey. Exp Brain Res. 62:215–223.

Munsch T, Yanagawa Y, Obata K, Pape HC. 2005. Dopaminergic control of local interneuron activity in the thalamus. Eur J Neurosci. 21:290–294.

Olszewski J. 1952. The thalamus of the Macaca mulatta. An atlas for use with the stereotaxic instrument. Basel (Switzerland): Karger.

Ottersen OP, Storm-Mathisen J. 1984. GABA-containing neurons in the thalamus and pretectum of the rodent. An immunocytochemical study. Anat Embryol (Berl). 170:197–207.

Papadopoulos GC, Parnavelas JG. 1990. Distribution and synaptic organization of dopaminergic axons in the lateral geniculate nucleus of the rat. J Comp Neurol. 294:356–361.

Paxinos G, Watson C. 1986. The rat brain in stereotaxic coordinates. Sydney (Australia): Academic Press.

Peters A, Palay SL, Webster HD. 1991. The fine structure of the nervous system. New York: Oxford University Press.

Pickel VM, Nirenberg MJ, Milner TA. 1996. Ultrastructural view of central catecholaminergic transmission: immunocytochemical localization of synthesizing enzymes, transporters and receptors. J Neurocytol. 25:843–856.

Pifl C, Bertel O, Schingnitz G, Hornykiewicz O. 1990. Extrastriatal dopamine in symptomatic and asymptomatic rhesus monkeys treated with 1-methyl-4-phenyl-1,2,3,6-tetrahydropyridine (MPTP). Neurochem Int. 17:263–270.

Pifl C, Caron MG. 2002. The dopamine transporter: molecular biology, pharmacology and genetics. In: Di Chiara G, editor. Dopamine in the CNS I. Berlin: Springer. p. 257–297.
Pifl C, Schingnitz G, Hornykiewicz O. 1991. Effect of 1-methyl-4-phenyl-1,2,3,6-tetrahydropyridine on the regional distribution of brain monoamines in the rhesus monkey. Neuroscience. 44:591–605.
Preuss TM, Goldman-Rakic PS. 1987. Crossed corticothalamic and thalamocortical connections of macaque prefrontal cortex. J Comp Neurol. 257:269–281.
Rausell E, Jones EG. 1991. Histochemical and immunocytochemical compartments of the thalamic VPM nucleus in monkeys and their relationship to the representational map. J Neurosci. 11:210–225.
Reiner A. 1994. Catecholaminergic innervation of the basal ganglia in mammals: anatomy and functin. In: Smeets WJAJ, Reiner A, editors. Phylogeny and development of catecholamine systems in the CNS of vertebrates. Cambridge (UK): Cambridge University Press. p. 247–272.
Sánchez-González MA, García-Cabezas MA, Rico B, Cavada C. 2005. The primate thalamus is a key target for brain dopamine. J Neurosci. 25:6076–6083.
Schwartz ML, Dekker JJ, Goldman-Rakic PS. 1991. Dual mode of corticothalamic synaptic termination in the mediodorsal nucleus of the rhesus monkey. J Comp Neurol. 309:289–304.
Schwartz ML, Mrzljak L. 1993. Cholinergic innervation of the mediodorsal thalamic nucleus in the monkey: ultrastructural evidence supportive of functional diversity. J Comp Neurol. 327:48–62.
Shu S, Ju G, Fan L. 1988. The glucose oxidase-DAB-nickel method in peroxidase histochemistry of the nervous system. Neurosci Lett. 85:169–171.
Smits M, Peeters RR, van Hecke P, Sunaert S. 2007. A 3 T event-related functional magnetic resonance imaging (fMRI) study of primary and secondary gustatory cortex localization using natural tastants. Neuroradiology. 49:61–71.
Takada M, Campbell KJ, Moriizumi T, Hattori T. 1990. On the origin of the dopaminergic innervation of the paraventricular thalamic nucleus. Neurosci Lett. 115:33–36.
Verney C. 1999. Distribution of the catecholaminergic neurons in the central nervous system of human embryos and fetuses. Microsc Res Tech. 46:24–47.
Williams SM, Goldman-Rakic PS. 1993. Characterization of the dopaminergic innervation of the primate frontal cortex using a dopamine-specific antibody. Cereb Cortex. 3:199–222.
Williams SM, Goldman-Rakic PS. 1998. Widespread origin of the primate mesofrontal dopamine system. Cereb Cortex. 8: 321–345.
Zoli M, Torri C, Ferrari R, Jansson A, Zini I, Fuxe K, Agnati LF. 1998. The emergence of the volume transmission concept. Brain Res Rev. 26:136–147.